

## Case Report

# A Climate-Mathematical Clustering of Rainfall Stations in the Río Bravo-San Juan Basin (Mexico) by Using the Higuchi Fractal Dimension and the Hurst Exponent

Francisco Gerardo Benavides-Bravo <sup>1</sup>, Dulce Martínez-Peon <sup>2</sup>, Ángela Gabriela Benavides-Ríos <sup>1</sup>,  
Otoniel Walle-García <sup>3</sup>, Roberto Soto-Villalobos <sup>3</sup> and Mario A. Aguirre-López <sup>1,\*</sup><sup>†</sup>

<sup>1</sup> Department of Basic Sciences, Instituto Tecnológico de Nuevo León, Tecnológico Nacional de México, Guadalupe 67170, Mexico; francisco.bb@nuevoleon.tecnm.mx (F.G.B.-B.); angela.br@nuevoleon.tecnm.mx (Á.G.B.-R.)

<sup>2</sup> Department of Electrical and Electronics Engineering, Instituto Tecnológico de Nuevo León, Tecnológico Nacional de México, Guadalupe 67170, Mexico; dulce.mp@nuevoleon.tecnm.mx

<sup>3</sup> Departamento de Ciencias Básicas, Facultad de Ciencias de la Tierra, Universidad Autónoma de Nuevo León, Linares 67700, Mexico; otoniel.wallega@uanl.edu.mx (O.W.-G.); roberto.sotovll@uanl.edu.mx (R.S.-V.)

\* Correspondence: mariao1906@gmail.com

† Current address: Facultad de Ciencias en Física y Matemáticas, Universidad Autónoma de Chiapas, Tuxtla Gutiérrez 29050, Mexico.



**Citation:** Benavides-Bravo, F.G.; Martínez-Peon, D.; Benavides-Ríos, Á.G.; Walle-García, O.; Soto-Villalobos, R.; Aguirre-López, M.A. A Climate-Mathematical Clustering of Rainfall Stations in the Río Bravo-San Juan Basin (Mexico) by Using the Higuchi Fractal Dimension and the Hurst Exponent. *Mathematics* **2021**, *9*, 2656. <https://doi.org/10.3390/math9212656>

Academic Editors: Theodore E. Simos and Charampos Tsitouras

Received: 17 September 2021

Accepted: 15 October 2021

Published: 20 October 2021

**Publisher's Note:** MDPI stays neutral with regard to jurisdictional claims in published maps and institutional affiliations.



**Copyright:** © 2021 by the authors. Licensee MDPI, Basel, Switzerland. This article is an open access article distributed under the terms and conditions of the Creative Commons Attribution (CC BY) license (<https://creativecommons.org/licenses/by/4.0/>).

**Abstract:** When conducting an analysis of nature's time series, such as meteorological ones, an important matter is a long-range dependence to quantify the global behavior of the series and connect it with other physical characteristics of the region of study. In this paper, we applied the Higuchi fractal dimension and the Hurst exponent (rescaled range) to quantify the relative trend underlying the time series of historical data from 17 of the 34 weather stations located in the Río Bravo-San Juan Basin, Mexico; these data were provided by the National Water Commission (CONAGUA) in Mexico. In this way, this work aims to perform a comparative study about the level of persistency obtained by using the Higuchi fractal dimension and Hurst exponent for each station of the basin. The comparison is supported by a climate clustering of the stations, according to the Köppen classification. Results showed a better fitting between the climate of each station and its Higuchi fractal dimension obtained than when using the Hurst exponent. In fact, we found that the more the aridity of the zone the more the persistency of rainfall, according to Higuchi's values. In turn, we found more relation between the Hurst exponent and the accumulated amount of rainfall. These are relations between the climate and the long-term persistency of rainfall in the basin that could help to better understand and complete the climatological models of the study region. Trends between the fractal exponents used and the accumulated annual rainfall were also analyzed.

**Keywords:** rainfall data; time series; long-range dependence; Higuchi fractal dimension; Hurst exponent; clustering; climate; Köppen climate classification; Monterrey Metropolitan Area (MMA)

## 1. Introduction

Climate changes dynamically over time, and factors like the increase of population, cattle and agriculture, industry, among others contribute to these changes [1]. Climate changes could increase or decrease precipitations, which provoke floods or droughts [2], changes in plant and bacterial diversity [3], and soil sealing [4]. Moreover, global warming has been presented as a concerning factor, in recent years, that have increased heavy precipitations [5].

Rainfall characterization is considered as an useful information to make decisions about water resource availability, agricultural production, or prediction of precipitations [6,7]. Due to the complex nature of rainfall phenomena, some studies suggest obtaining characteristics using fractal algorithms, first because of their cyclic behavior over long-range time series [8],

and second, because of the lack of regularity of occurrence of the phenomena [9,10]. Indeed, since decades ago, some studies have used algorithms based on fractals to characterize rainfalls, predict climatology and behavior of water processes [11–17], some of which have been dealt with the Hurst exponent ( $H$ ) or the Higuchi fractal dimension ( $HFD$ ) [16,18]. In addition, such methodologies have been used to quantify the persistency, anti-persistency or randomness of the data from the different weather stations with monthly records, in different periods [10,19].

The measure of the persistency of the series in the Hurst exponent consists of a dimensionless scale between 0 and 1 so that the closer the value is to 1, the more persistency [20]. In detail, if  $H < 0.5$ , the time series presents anti-persistency; if  $H = 0.5$ , it presents a behaviour similar to Gaussian noise; and  $H > 0.5$ , the time series presents persistency. In turn,  $HFD$  calculates persistency by values going from 1 (anti-persistency in the series) to 2 (persistency) [21].

In this context, the most used method to calculate Hurst exponent is rescaled range because of their simplicity to calculate it using statistical tools, [19,22], however, it has some disadvantages against trends, Kantelhardt et al. [23]. Rescaled range is not the only method to calculate Hurst exponent, wavelets [24], power spectrum [25] and Anny's Lloyd [26] methods have been also reported. Rehman and Siddiqi [16] used a methodology based on Hurst exponent and wavelets to calculate persistency of climate predictability indices, founding that precipitation and temperature indices are independent. Chandrasekaran et al. [18] used  $H$  for rainfall prediction, concluding that such index must be close to 1 for obtaining an accurate forecast.

Moreover, Kalauzi et al. [27] calculated fractal dimension (FD) in rainfall time series using  $HFD$  with Fast Fourier Transform (FFT) to determine tendency of rainfalls of two regions. Ciobotaru et al. [28] related temperature-humidity index oscillations with  $HFD$  to calculate the impact on tourism activity.

The Río Bravo-San Juan (RBSJ) Basin covers an area of 34,000 km<sup>2</sup> within the Mexican States of Coahuila, Nuevo León, and Tamaulipas. It is located in the northeastern region of Mexico. RBSJ Basin belongs to the RH24 hydrological region, one of the largest watershed areas. RH24 is characterized to be constantly hit by hurricanes and heavy rainfalls that provoke dangerous landslides [29]. The main stem of RBSJ Basin is named Río San Juan, but other smaller branches such as Río Pilón, Río Salinas, Río Pesquería, Río Santa Catarina, and Río Ramos are important tributaries [30]. Figure 1 illustrates its three main types of climates according to the National Commission for the Knowledge and Use of Biodiversity (CONABIO) of Mexico [31]: hot semi-arid, hot desert and humid sub-tropical. In general semi-arid to arid (i.e., desert) climates dominate in the RBSJ Basin. These climatic conditions joined to the annual-cyclical patterns of rainfall [32], create an unstable water supply for the region [33]. The humid sub-tropical climate covers the majority of Monterrey Metropolitan Area (MMA), which is one of the third main metropolises in Mexico, and concentrates 90% of the population of Nuevo León. The rapid increasing water demand for industrial, agricultural and domestic usage in the MMA has stressed the current water supply, while severe droughts continue to exhaust the region's known reserves. For these reasons and also because of the constant pollution in the MMA [34], this region must be analyzed in order to prevent possible events that could cause disasters for the population.

In this work, time series obtained from 17 of the 34 weather stations of RBSJ Basin were analyzed. We investigated the underlying long-term dependency behavior patterns of those series through the Higuchi fractal dimension ( $HFD$ ) and the rescaled range version of the Hurst exponent ( $Hrs$ ). Then, we related our comparative analysis with the different types of climate of the basin. Finally, a classification or clustering of the stations with similar behaviors was carried out in order to discuss about the climatic characteristics of the region, the amount of rainfall per year, and their relation with the rainfall persistency. The structure of the paper is as follows: Section 2 describes the methodology, from the way to obtain the time series to the building of the fractal exponents used; Section 3 shows our

results, including the clustering of the stations; finally, we interpret and discuss our results in Section 4, and show some concluding remarks in Section 5.

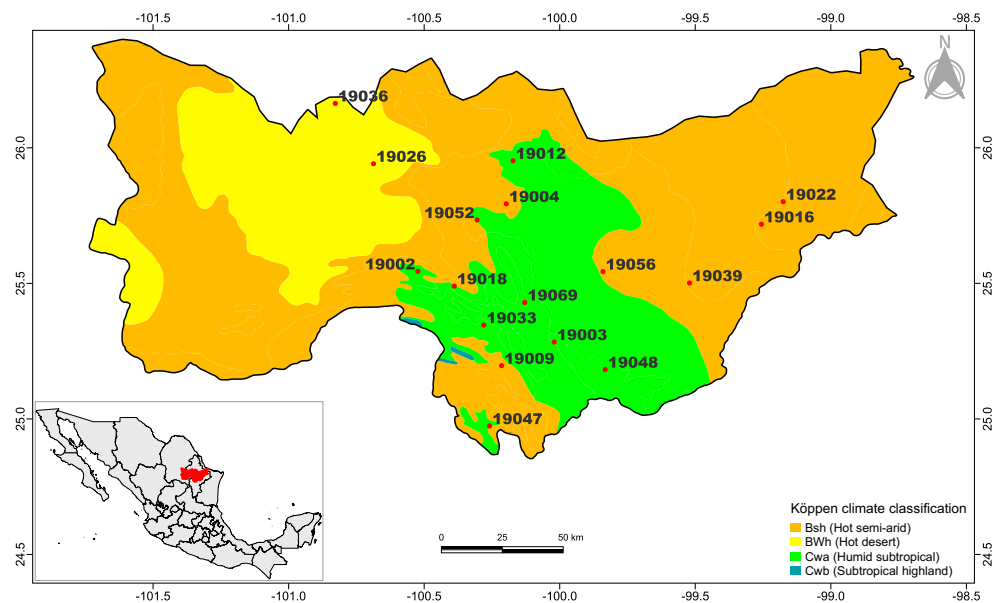


**Figure 1.** CONABIO’s clustering of Río Bravo-San Juan Basin, Mexico, by using the Köppen climate classification [35].

## 2. Methodology

In our case study, 17 of 34 weather stations of the RBSJ Basin were analyzed. They are located in the northeast region of Mexico, covering an approximate area of 29,420 km<sup>2</sup>. The selected stations were those having uninterrupted records within the period of years 1964–2016, this in order to have homogeneity in the quality of the data for the time series of all the stations. The region of study, including the 17 georeferenced stations are shown in Figure 1, tagged by their station number. For each weather station we have information of the month-accumulated rainfall, which leads to 636 data points for each series. We used monthly data because it is the available public information reported by CONAGUA.

### 2.1. Hurst Exponent (Hrs)

The version of the Hurst exponent we consider is the rescaled range, in which the information of each station is represented as vectors  $(X_k)_{k \in 1:N}$ , where  $N$  is the number of months considered for the analysis. Each vector  $(X_k)$  is divided into a set of  $d$ -subseries of shorter time with the same quantity of data, such that all the  $n$ -th subseries,  $n = 1, 2, \dots, d$ , have a length of  $m$ . Then, according to [36,37], the following steps are carried out for each subseries:

1. Calculate the mean  $M_n$  and the standard deviation  $S_n$  of the subseries.
2. Determine the variation  $V_{in}$  of each term with respect to the mean:

$$V_{in} = X_{in} - M_n, \text{ for } i = 1, \dots, m \tag{1}$$

3. Obtain the accumulated sum of variation until the  $i$ th-term:

$$Y_{in} = \sum_{j=1}^i V_{jn}, \text{ for } i = 1, \dots, m \tag{2}$$

4. Calculate the range of each subseries:

$$R_n = \max_{j=1:m} Y_{jn} - \min_{j=1:m} Y_{jn} \tag{3}$$

5. Normalize the calculated ranges (this is why it is called rescaled range):

$$R_n / S_n \tag{4}$$

6. Once this is done for each subseries of length  $m$ , they are averaged:

$$\langle \widehat{R_n / S_n} \rangle = \frac{1}{d} \sum_{n=1}^d \frac{R_n}{S_n} \tag{5}$$

7. Finally, the relation of the statistic  $\langle \widehat{R_n / S_n} \rangle$  is given by the following power law:

$$\langle \widehat{R/S} \rangle_m \approx cm^H \tag{6}$$

where  $H$  refers to  $Hrs$  and its a dimensionless number, and  $c > 0$  is a constant.

In this way,  $Hrs$  can be estimated by rewriting (7) in logarithmic terms:

$$\log_{10} \langle \widehat{R/S} \rangle_m = \log_{10}(c) + H \log_{10}(m), \tag{7}$$

so that  $Hrs$  is the slope of the straight line. In this work, we used a total of  $d = 53$  partitions, each of them with a length of  $m = 12$  months.

### 2.2. Higuchi Fractal Dimension (HFD)

Higuchi fractal dimension (HFD) approximates the fractal dimension in a similar way to  $Hrs$ , in the sense of dividing the total time series in windows, however, their procedure are some different. For a time series  $X$ , with  $N$  data points [38],

$$L_m(k) = \frac{N - 1}{\lfloor \frac{N-m}{k} \rfloor k^2} \sum_{i=1}^{\lfloor \frac{N-m}{k} \rfloor} |X_N(m + ik) - X_N(m + (i - 1)k)| \tag{8}$$

expresses the fractal length of the subseries  $X_k^m$ , where  $k \in \{1, \dots, k_{max}\}$  indicates the  $k$ -th time,  $m \in \{1, \dots, k\}$  is the interval time of that subseries, and  $k_{max}$  is the total number of subseries used. In this work, we used  $k_{max} = 8$ , which is a significant number about an intermediate value between the Köppen classification by semesters [35] and the annual periodicity of the phenomenon in the region [37]. In addition, we carried out the calculation of HFD with several  $k_{max}$ , obtaining that  $k_{max} = 8$  gave the best relation between HFD and climate in terms of better limits between clusters, see Table A1 in Appendix A.

Thus, the total fractal length  $L(k)$  is defined as the mean of all the  $L_m(k)$ 's, so that

$$L(k) = \frac{1}{k} \sum_{m=1}^k L_m(k) \tag{9}$$

In this way, HFD is the slope  $F$  (dimensionless) that fits to the equation

$$\log_{10}(L(k)) = \log_{10}(b) + F \log_{10} \left( \frac{1}{k} \right), \tag{10}$$

where  $b > 0$  is a constant.

### 3. Results

For illustration of the general behaviour, time series of three representatives rain-fall stations (Allende, El Cuchillo and La Popa) are plotted in Figure 2, from 1964 to 2016. In this sense, Allende represents the humid subtropical climate ( $Cwa$ ), whereas El Cuchillo and La Popa represent the arid climates, namely, hot semi-arid ( $Bsh$ ) and hot desert ( $BWh$ ), respectively.

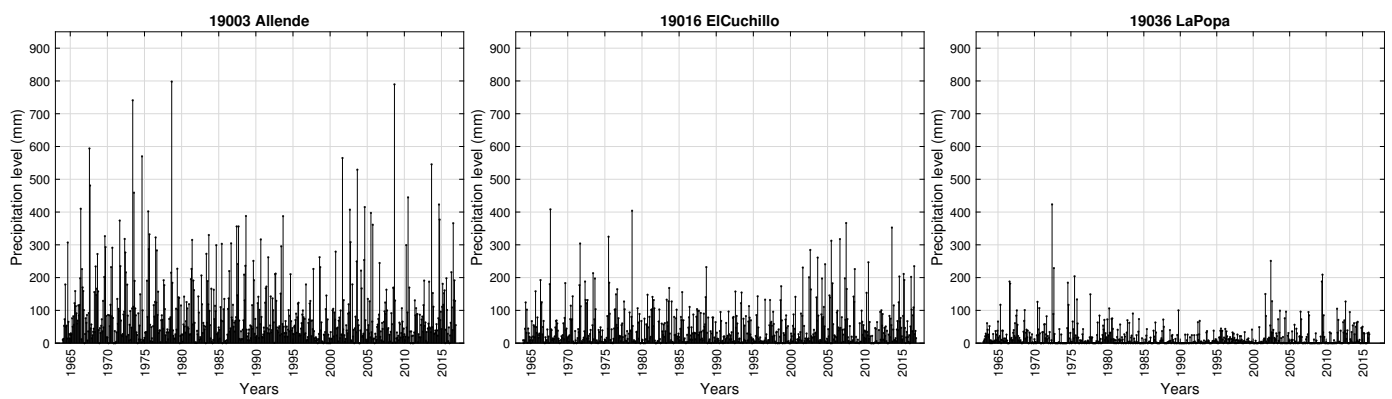


Figure 2. Time series of the stations Allende, El Cuchillo and La Popa.

Figure 3 shows the linear adjustments applied to Equation (7) for the selected stations. The calculation of the Hurst exponents was made by means of the least squares method. The value of the slope of the curve fitted is  $Hrs$ .

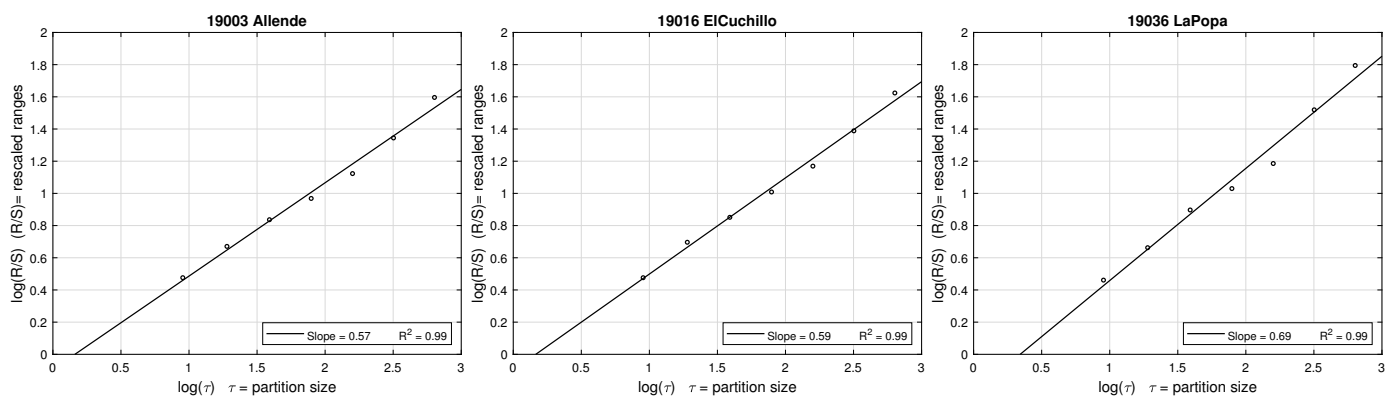


Figure 3. Calculation of  $Hrs$  by fitting the slope  $H$  from Equation (7), obtaining the coefficient of determination  $R^2$  when considering  $d = 53$ ,  $m = 12$ , which leads to seven data points to fit.

In turn, Figure 4 shows the linear adjustments applied to Equation (10), in order to perform the calculation of  $HFD$  for the selected stations, by means of the least squares method. The value of the slope of the curve fitted is  $HFD$ .

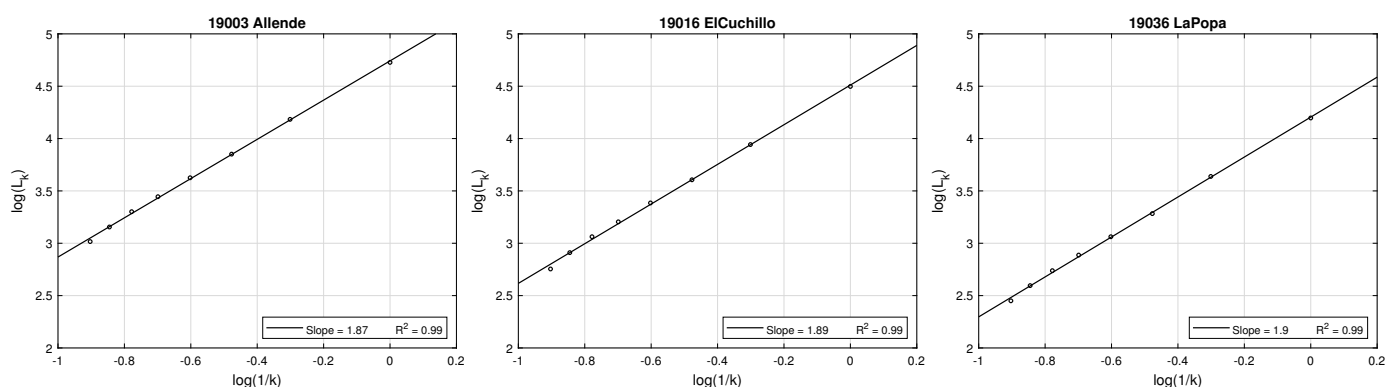


Figure 4. Calculation of  $HFD$  by fitting the slope  $F$  from Equation (10), obtaining the coefficient of determination  $R^2$  when considering  $k_{max} = 8$ , i.e., eight data points to fit.

Table 1 contains the summary of the adjustments carried out for all the stations analyzed. For each station, the table shows its number, name, coordinates (latitude and longitude), the obtained values of  $Hrs$  and  $HFD$ , accumulated annual rainfall (A.A.R.) in mm, and climate (with colors). Results are shown in an ascending order according to the

obtained value of *HFD*. All the values of *Hrs* and *HFD* were calculated up to the second decimal place as there is no significance from the third place [39].

**Table 1.** Characteristics and results for the 17 stations analyzed. Climate is shown by the corresponding color taken from the CONABIO's clustering that uses the Köppen climate classification, see Figure 1. Rows follow an ascending order with respect to the value of *HFD*.

Station	Name	Latitude	Longitude	<i>Hrs</i>	<i>HFD</i>	A.A.R.	Climate
19002	Agua Blanca	25.5442	−100.5231	0.62	1.78	614	<i>Cwa</i>
19018	El Pajonal	25.4897	−100.3889	0.50	1.79	557	<i>Cwa</i>
19069	La Boca	25.4294	−100.1289	0.48	1.81	1098	<i>Cwa</i>
19033	Laguna de Sánchez	25.3461	−100.2800	0.57	1.81	737	<i>Cwa</i>
19047	Mimbres	24.9739	−100.2586	0.54	1.82	676	<i>Cwa</i>
19009	Casillas	25.1964	−100.2142	0.48	1.82	590	<i>Bsh</i>
19039	Las Enramadas	25.5014	−99.5214	0.62	1.85	688	<i>Bsh</i>
19012	Ciénega de Flores	25.9522	−100.1722	0.70	1.86	647	<i>Cwa</i>
19003	Allende	25.2836	−100.0203	0.57	1.87	1091	<i>Cwa</i>
19048	Montemorelos	25.1819	−99.8322	0.50	1.87	904	<i>Cwa</i>
19052	Monterrey	25.7336	−100.3047	0.56	1.87	688	<i>Cwa</i>
19004	Apodaca	25.7936	−100.1972	0.48	1.88	566	<i>Bsh</i>
19016	El Cuchillo	25.7181	−99.2558	0.58	1.89	573	<i>Bsh</i>
19022	General Bravo	25.8014	−99.1756	0.62	1.89	593	<i>Bsh</i>
19056	San Juan	25.5433	−99.8403	0.53	1.89	731	<i>Bsh</i>
19036	La Popa	26.1639	−100.8278	0.71	1.90	246	<i>BWh</i>
19026	Icamole	25.9411	−100.6869	0.63	1.92	210	<i>BWh</i>

#### 4. Discussion

Accumulated rainfall per month are shown in time series of Figure 2. The amount and dispersion of rainfall are larger for Allende, which belongs to *Cwa* than for El Cuchillo and La Popa, which belong to more arid and hotter climates, *Bsh* and *BWh*, respectively.

Table 1 shows the persistency level obtained by *Hrs* and *HFD*, and relates their order with the climate clustering of the region provided by the Köppen classification. *Hrs* and *HFD* were calculated by fitting the illustrations in Figures 3 and 4, following their respective procedures of Section 2. As seen in Table 1, values of *Hrs* go from 0.48 to 0.71, i.e., about 0.23 units in range, whereas *HFD* goes from 1.78 to 1.92, having a range of 0.14 units. Instead of this, *HFD* fits better to the clustering of climates than *Hrs*. With the exception of Casillas and Las Enramadas, it is seen that  $HFD \in [1.78, 1.87]$  correspond to the *Cwa*, while  $HFD \in [1.88, 1.89]$  correspond to *Bsh*, and  $HFD \in [1.90, 1.92]$  correspond to *BWh*. Moreover, station Casillas is very close the border between *Cwa* and *Bsh* geographical zones, see Figure 1. This could suggest a relation between aridity and long-term memory of rainfall for this region study. In fact, there is a precedent that supports such assumption, in which there was found more persistency in rainfall time series associated to more arid zones of the Sahel region in Africa, although persistency was also found in subtropical areas [40]; nevertheless, the amount of rainfall is only considered for the internal classification of arid climates (type *B*), according to Köppen [35] in which the A.A.R. and its distribution throughout the year define the sub-climates.

Then, our results of A.A.R. in Table 1 relate to the climate in an inverse way than *HFD*, so that, the more the amount of rainfall the more humidity. Similarly to *HFD*, the border between *BWh* and *Bsh* is well identified by the amount of rainfall (about 300 mm of separation), but three stations do not permit a compact clustering for separating *Bsh* (572–731 mm) from *Cwa* (557–1098 mm), namely, Las Enramadas, and San Juan and El Pajonal. The two latter stations are also located in a geographical border of climates, see Table 1 and Figure 1. In this way, Las Enramadas is the only station, geographically far to the borders, that does not fit to the relations *HFD*-climate and A.A.R.-climate.

We associate the difference in fit of each model to the way in which they define or calculate fractality. Namely, *HFD* fits better because each *i*-measure consists of the difference between rainfall of two timely consecutive *i*-subseries, in Equation (8), which agrees with the division by seasons in the arid classification of Köppen. In contrast to this, *Hrs* measures the range of each *n*-subseries to calculate fractality, in Equation (3).

Regarding our obtained values of Hurst, all of them are higher than 0.5 and do not have a direct relation with climate, as mentioned before. This agrees with the results of López-Lambrano et al. [24], who found persistency in their precipitation series, obtaining Hurst values from 0.5 to 0.9, but contrasts with Kantelhardt et al. [23], who did not find relation between hydrologic persistence and Hurst (values lower than 0.5). Such observations could be related to two main reasons. On the one hand, there is the climate-physical part, which deals with the fact that López-Lambrano et al. [24] analyzed a very similar region about climate than ours, while Kantelhardt et al. [23] studied three very different regions to our work. On the other hand, there is the climate-methodological part, since the studies mentioned in Kantelhardt et al. [23] dealt with large time series of more than 100 years, in which climate could have changed and led to low values of persistence. In fact, López-Lambrano et al. [24] found a decrease in the values of *Hrs* by increasing the length of their time series from 5 to 30 years.

Additionally, we measured and plotted the relations *Hrs*-A.A.R. and *HFD*-A.A.R. in Figure 5. Despite a clear trend in both curves, there is a lot of dispersion indicating a weak relation ( $R^2 \approx 0.1$  for *HFD*-A.A.R. relation and  $R^2 \approx 0.3$  for *Hrs*-A.A.R. ). In turn, relation *HFD* – *HRS* is also weak ( $R^2 \approx 0.1$ ), see Figure 6. We associated the larger dispersion in our curves to the predominance of the subtropical climate of the region since arid climates possess more roughness, as mentioned in [41].

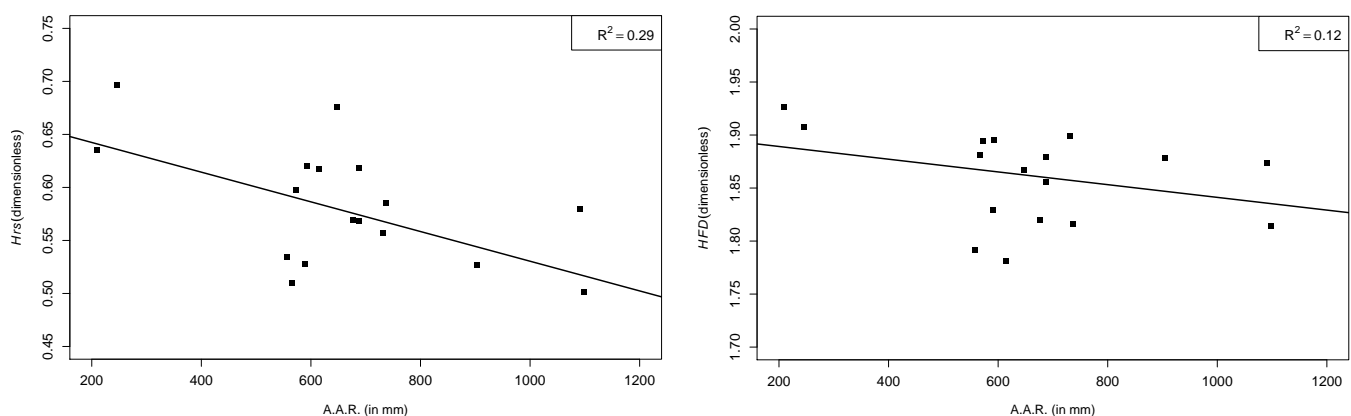


**Figure 5.** Relation between fractal exponents and A.A.R., showing their coefficients of determination ( $R^2$ ) of the fits.

Therefore, our final observations are focused on three main points:

- The RBSJ Basin is a complex region composed by mainly three climates *Cwa*, *Bsh* and *BWh*. Its complexity consists of a geographical mixing of those climates, which makes it difficult to perform a good interpolation by traditional techniques like the Köppen climate classification and A.A.R., and even by more complex techniques like *Hrs* and *HFD*. Indeed, about five weather stations are located in the border of zones cataloged as subtropical (*Cwa*) and semi-arid (*Bsh*) climates.
- Nevertheless, fractal exponents have shown to have a relation with climates (*HFD*) and in a weaker sense with A.A.R., which have been reported previously in regions with similar climates [40,41]. In this manner, our study aims to suggest the use of those fractal exponents as an alternative way to understand and complete the climate maps of the region study, positioning *HFD* as a measure of classification at the same level of A.A.R., and having as an advantage the memory of the time that the method possesses.
- As future research, we propose to determine the relation between *HFD* and the weather to a regional scale, extending this to east and north, where the weather is

similar, and considering other regions like Veracruz, Tabasco and Chiapas, which are southeast Mexico's states where the weather is different to the studied region. In this form, it could be possible to analyze if the correlation between *HFD* and the weather change lightly or radically. In the first case, the relation will be not a regional case, and it will derive to a larger scale.

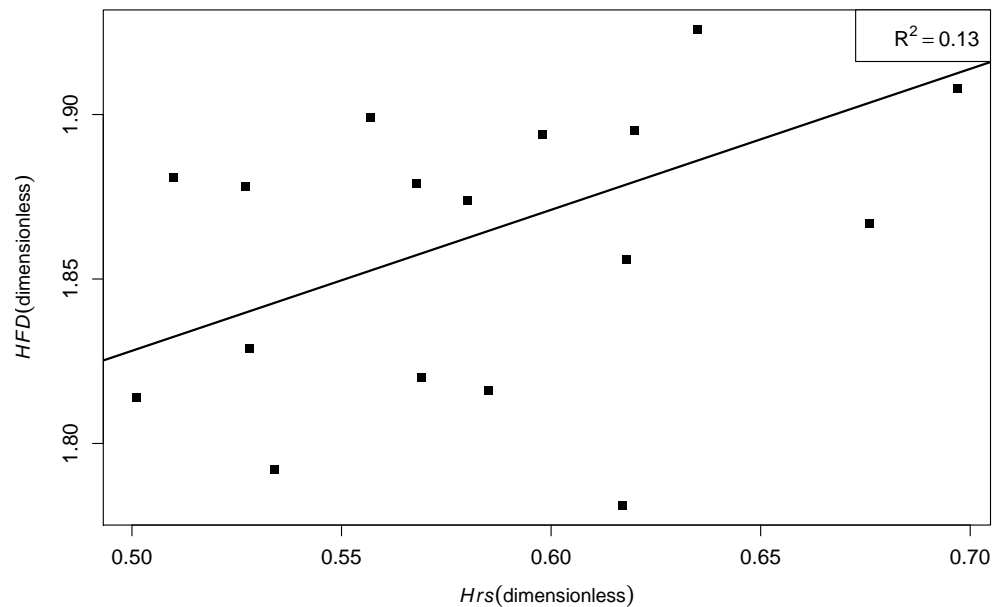


**Figure 6.** Relation between fractal exponents, showing the coefficients of determination ( $R^2$ ) of the fit.

## 5. Conclusions

This work aimed to analyze the dependency of long-range time series by using Hurst Exponent and Higuchi Dimensional Fractal. We found a strong dependency between *HFD* and the climates, but not for Hurst Exponent and the climates.

We evaluated the persistency of 17 rainfall time series of the RBSJ Basin in Mexico utilizing *Hrs* and *HFD*, and compared their values with the climate classification proposed by the CONABIO, which uses the Köppen climate classification. We found more relation between the clusters formed by the Köppen classification and the obtained Higuchi's values.

In detail, our Higuchi's results suggest that the persistency of the series increase with the aridity of the zone, so that, the stations located at the humid subtropical zone have the lowest *HFD*'s values,  $HFD \in [1.78, 1.87]$ ; those located at the hot semi-arid zone have  $HFD \in [1.88, 1.89]$ ; and finally, the hot desert zone contains the stations with the highest values  $HFD \in [1.90, 1.92]$ . This suggests that the arid zones of the study region have more persistent rainfalls, although not necessarily predictable, which has been reported previously in region studies with similar climates [40,41]. In turn, *Hrs* did not fit very well to the climates and had a weak relation with the A.A.R.

In this way, we concluded that *HFD* is a powerful indicator for analyzing rainfall time series that can help to understand the climates of the case study in terms of combining a climate classification with a mathematical measure. Thus, the climate-mathematical clustering technique that we present is a primary study that quantifies the limits of the climatic zones within the RBSJ Basin, which could help to complete or redefine the climatological models of the study region.

**Author Contributions:** Conceptualization, F.G.B.-B. and O.W.-G.; methodology, F.G.B.-B. and R.S.-V.; software, F.G.B.-B., R.S.-V., Á.G.B.-R. and O.W.-G.; validation, F.G.B.-B., R.S.-V., D.M.-P. and M.A.A.-L.; formal analysis, F.G.B.-B., R.S.-V. and M.A.A.-L.; investigation, F.G.B.-B., R.S.-V. and D.M.-P.; resources, F.G.B.-B., R.S.-V. and D.M.-P.; data curation, F.G.B.-B. and Á.G.B.-R.; writing—original draft preparation, F.G.B.-B., R.S.-V., D.M.-P. and M.A.A.-L.; writing—review and editing, F.G.B.-B., R.S.-V., D.M.-P. and M.A.A.-L.; visualization, F.G.B.-B., R.S.-V., Á.G.B.-R., O.W.-G. and M.A.A.-L.; critical revision for important intellectual content, F.G.B.-B., R.S.-V., D.M.-P., Á.G.B.-R. and M.A.A.-L.; supervision, F.G.B.-B.; project administration, M.A.A.-L.; and final approval of the version to be published, F.G.B.-B., R.S.-V., Á.G.B.-R., D.M.-P., M.A.A.-L. and O.W.-G. All authors have read and agreed to the published version of the manuscript.

**Funding:** This research was fully funded by the Tecnológico Nacional de México/Instituto Tecnológico de Nuevo León.

**Institutional Review Board Statement:** Not applicable.

**Informed Consent Statement:** Not applicable.

**Data Availability Statement:** Data used in this work were provided, in a private way, by CONAGUA. However, similar data are available at Google Earth, installing the extensions of rainfall stations in the format *.kmz*.

**Acknowledgments:** We appreciate to the CONAGUA for providing the data, specially to Doroteo Treviño Puente and Oscar Gutiérrez. We thank also to our universities for the support shown to this research throughout the current pandemic event COVID-19. Finally, we thank to the reviewers that took part in the reviewing process of this work; they helped us a lot to improve this research.

**Conflicts of Interest:** The authors declare no conflict of interest.

## Appendix A

**Table A1.** Results of *HFD* for the 17 stations analyzed with different  $k_{max}$ . Stations are shown in an ascendant order according to  $k_{max} = 8$ .

Station	Name	$k_{max} = 6$	7	8	9	10	11	12
19002	Agua Blanca	1.72	1.75	1.78	1.81	1.86	1.90	1.95
19018	El Pajonal	1.74	1.76	1.79	1.82	1.86	1.91	1.95
19069	La Boca	1.76	1.78	1.81	1.84	1.88	1.93	1.98
19033	Laguna De Sánchez	1.77	1.78	1.81	1.84	1.88	1.93	1.98
19047	Mimbres	1.76	1.78	1.82	1.85	1.88	1.91	1.95
19009	Casillas	1.78	1.80	1.82	1.86	1.89	1.93	1.98
19039	Las Enramadas	1.81	1.83	1.85	1.87	1.91	1.94	1.99
19012	Cienega De Flores	1.82	1.84	1.86	1.89	1.91	1.94	1.97
19003	Allende	1.83	1.85	1.87	1.89	1.91	1.94	1.99
19048	Montemorelos	1.84	1.85	1.87	1.89	1.91	1.94	1.98
19052	Monterrey	1.84	1.85	1.87	1.89	1.91	1.95	1.99
19004	Apodaca	1.84	1.86	1.88	1.89	1.91	1.94	1.97
19016	El Cuchillo	1.84	1.86	1.89	1.91	1.92	1.95	1.98
19022	General Bravo	1.85	1.86	1.89	1.91	1.92	1.94	1.97
19056	San Juan	1.85	1.87	1.89	1.90	1.92	1.95	1.98
19036	La Popa	1.87	1.88	1.90	1.91	1.93	1.95	1.97
19026	Icamole	1.91	1.91	1.92	1.93	1.93	1.94	1.97

## References

1. Trenberth, K. Changes in Precipitation with Climate Change. *Climate Change Research. Clim. Res.* **2011**, *47*, 123–138. [[CrossRef](#)]
2. Trenberth, K. *The Impact of Climate Change and Variability on Heavy Precipitation, Floods, and Droughts*; John Wiley & Sons, Ltd.: Hoboken, NJ, USA, 2008. [[CrossRef](#)]
3. Zhang, H.; Liu, H.; Zhao, J.; Wang, L.; Li, G.; Huangfu, C.; Wang, H.; Lai, X.; Li, J.; Yang, D. Elevated precipitation modifies the relationship between plant diversity and soil bacterial diversity under nitrogen deposition in *Stipa baicalensis* steppe. *Appl. Soil Ecol.* **2017**, *119*, 345–353. [[CrossRef](#)]

4. Assouline, S.; Mualem, Y. Modeling the dynamics of soil seal formation: Analysis of the effect of soil and rainfall properties. *Water Resour. Res.* **2000**, *36*, 2341–2350. [[CrossRef](#)]
5. Tabari, H. Climate change impact on flood and extreme precipitation increases with water availability. *Sci. Rep.* **2020**, *10*, 13768. [[CrossRef](#)]
6. Nathan, O.O.; Felix, N.K.; Milka, K.N.; Anne, M.; Noah, A.; Daniel, M.N. Suitability of different data sources in rainfall pattern characterization in the tropical central highlands of Kenya. *Heliyon* **2020**, *6*, e05375. [[CrossRef](#)]
7. Potter, N.J.; Chiew, F.H.S.; Charles, S.P.; Fu, G.; Zheng, H.; Zhang, L. Bias in dynamically downscaled rainfall characteristics for hydroclimatic projections. *Hydrol. Earth Syst. Sci.* **2020**, *24*, 2963–2979. [[CrossRef](#)]
8. Mandelbrot, B. Statistical Methodology for Nonperiodic Cycles: From the Covariance To R/S Analysis. In *Annals of Economic and Social Measurement, Volume 1, Number 3*; National Bureau of Economic Research, Inc.: Cambridge, MA, USA, 1972; pp. 259–290.
9. Hurst, H. A Suggested Statistical Model of some Time Series which occur in Nature. *Nature* **1957**, *180*, 494. [[CrossRef](#)]
10. Mandelbrot, B.B.; Wallis, J.R. Robustness of the rescaled range R/S in the measurement of noncyclic long run statistical dependence. *Water Resour. Res.* **1969**, *5*, 967–988. [[CrossRef](#)]
11. Breslin, M.; Belward, J. Fractal dimensions for rainfall time series. *Math. Comput. Simul.* **1999**, *48*, 437–446. [[CrossRef](#)]
12. Sivakumar, B. Is a chaotic multi-fractal approach for rainfall possible? *Hydrol. Process.* **2001**, *15*, 943–955. [[CrossRef](#)]
13. Matsoukas, C.; Islam, S.; Rodriguez-Iturbe, I. Detrended fluctuation analysis of rainfall and streamflow time series. *J. Geophys. Res. Atmos.* **2000**, *105*, 29165–29172. [[CrossRef](#)]
14. Olsson, J.; Niemczynowicz, J.; Berndtsson, R. Fractal analysis of high-resolution rainfall time series. *J. Geophys. Res. Atmos.* **1993**, *98*, 23265–23274. [[CrossRef](#)]
15. Palanikumar, R.; Sathyamoorthy, D. An alternative approach to characterize time series data: Case study on Malaysian rainfall data. *Chaos Solitons Fractals* **2006**, *27*, 511–518. [[CrossRef](#)]
16. Rehman, S.; Siddiqi, A. Wavelet based hurst exponent and fractal dimensional analysis of Saudi climatic dynamics. *Chaos Solitons Fractals* **2009**, *40*, 1081–1090. [[CrossRef](#)]
17. Mihailović, D.T.; Nikolić-Đorić, E.; Malinović-Milićević, S.; Singh, V.P.; Mihailović, A.; Stošić, T.; Stošić, B.; Drešković, N. The Choice of an Appropriate Information Dissimilarity Measure for Hierarchical Clustering of River Streamflow Time Series, Based on Calculated Lyapunov Exponent and Kolmogorov Measures. *Entropy* **2019**, *21*, 215. [[CrossRef](#)] [[PubMed](#)]
18. Chandrasekaran, S.; Poomalai, S.; Balamurali, S.; Sumila, S.; Keerthi, S.; Farveen, A. An Investigation on Relationship between Hurst exponent and Predictability of a Rainfall Time Series. *Meteorol. Appl.* **2019**, *26*, 511–519. [[CrossRef](#)]
19. Pal, S.; Dutta, S.; Nasrin, T.; Chattopadhyay, S. Hurst exponent approach through rescaled range analysis to study the time series of summer monsoon rainfall over northeast India. *Theor. Appl. Climatol.* **2020**, *142*, 581–587. [[CrossRef](#)]
20. Hurst, H.E. Long-Term Storage Capacity of Reservoirs. *Trans. Am. Soc. Civ. Eng.* **1951**, *116*, 770–799. [[CrossRef](#)]
21. Voss, R.F. Random Fractals: Characterization and measurement. In *Scaling Phenomena in Disordered Systems*; Pynn, R., Skjeltorp, A., Eds.; Springer: Boston, MA, USA, 1991; pp. 1–11. [[CrossRef](#)]
22. Mukherjee, S. Contrasting predictability of summer monsoon rainfall ISOs over the northeastern and western Himalayan region: An application of Hurst exponent. *Meteorol. Atmos. Phys.* **2019**, *131*, 55–61. [[CrossRef](#)]
23. Kantelhardt, J.; Koscielny-Bunde, E.; Rybski, D.; Braun, P.; Bunde, A.; Havlin, S. Long-term persistence and multifractality of precipitation and river runoff records. *J. Geophys. Res.* **2006**, *111*. [[CrossRef](#)]
24. López-Lambrano, A.A.; Fuentes, C.; López-Ramos, A.A.; Mata-Ramírez, J.; López-Lambrano, M. Spatial and temporal Hurst exponent variability of rainfall series based on the climatological distribution in a semiarid region in Mexico. *Atmósfera* **2018**, *31*, 199–219. [[CrossRef](#)]
25. Sun, J.; Wang, X.; Shahid, S. Precipitation and runoff variation characteristics in typical regions of North China Plain: A case study of Hengshui City. *Theor. Appl. Climatol.* **2020**, *142*, 971–985. [[CrossRef](#)]
26. Anis, A.A.; Lloyd, E.H. The Expected Value of the Adjusted Rescaled Hurst Range of Independent Normal Summands. *Biometrika* **1976**, *63*, 111–116. [[CrossRef](#)]
27. Kalauzi, A.; Čukić, M.; Millán, H.; Bonafoni, S.; Biondi, R. Comparison of fractal dimension oscillations and trends of rainfall data from Pastaza Province, Ecuador and Veneto, Italy. *Atmos. Res.* **2009**, *93*, 673–679. [[CrossRef](#)]
28. Ciobotaru, A.M.; Andronache, I.; Dey, N.; Petralli, M.; Mansouri Daneshvar, M.R.; Wang, Q.; Radulovic, M.; Pintilii, R. Temperature-Humidity Index described by fractal Higuchi Dimension affects tourism activity in the urban environment of Focșani City (Romania). *Theor. Appl. Climatol.* **2019**, *136*, 1009–1019. [[CrossRef](#)]
29. Sanchez-Castillo, L.; Kubota, T.; Silva, I.C. Critical Rainfall for the Triggering of Sediment Related Disasters under the Urban Forest Development in Nuevo Leon, Mexico. *Int. J. Ecol. Dev.* **2015**, *30*, 1–10.
30. Nívar Cháidez, J. Water Scarcity and Degradation in the Rio San Juan Watershed of Northeastern Mexico. *Front. Norte* **2011**, *46*, 125–150.
31. García, E. Comisión Nacional para el Conocimiento y Uso de la Biodiversidad (CONABIO). Climas (Clasificación de Koppen). 1998. Available online: <http://www.conabio.gob.mx/informacion/gis/> (accessed on 1 September 2021).
32. Benavides-Bravo, F.G.; Soto-Villalobos, R.; Cantú-González, J.R.; Aguirre-López, M.A.; Benavides-Ríos, A.G. A Quadratic-Exponential Model of Variogram Based on Knowing the Maximal Variability: Application to a Rainfall Time Series. *Mathematics* **2021**, *9*, 2466. [[CrossRef](#)]

33. Villanueva-Hernández, H.; Tovar-Cabañas, R.; Vargas-Castilleja, R. Classification of aquifers in the Mina field, Nuevo Leon, using geographic information systems. *Tecnol. Cienc. Agua* **2014**, *10*, 96–123. [[CrossRef](#)]
34. Benítez-García, S.E.; Kanda, I.; Wakamatsu, S.; Okazaki, Y.; Kawano, M. Analysis of Criteria Air Pollutant Trends in Three Mexican Metropolitan Areas. *Atmosphere* **2014**, *5*, 806–829. [[CrossRef](#)]
35. Köppen, W. Klassifikation der Klimate nach Temperatur, Niederschlag und Jahreslauf (Classification of climates according to temperature, precipitation and seasonal cycle). *Petermanns Geogr. Mitteilungen* **1918**, *64*, 193–203. 243–248.
36. Bassingthwaite, J.B.; Raymond, G.M. Evaluating rescaled range analysis for time series. *Ann. Biomed. Eng.* **1994**, *22*, 432–444. [[CrossRef](#)]
37. Benavides-Bravo, F.; Almaguer, F.; Soto-Villalobos, R.; Tercero-Gómez, V.; Morales-Castillo, J. Clustering of Rainfall Stations in RH-24 Mexico Region Using the Hurst Exponent in Semivariograms. *Math. Probl. Eng.* **2015**, *2015*, 629254. [[CrossRef](#)]
38. Higuchi, T. Approach to an irregular time series on the basis of the fractal theory. *Phys. D Nonlinear Phenom.* **1988**, *31*, 277–283. [[CrossRef](#)]
39. Bashan, A.; Bartsch, R.; Kantelhardt, J.W.; Havlin, S. Comparison of detrending methods for fluctuation analysis. *Phys. A Stat. Mech. Its Appl.* **2008**, *387*, 5080–5090. [[CrossRef](#)]
40. Nicholson, S.E. Revised Rainfall Series for the West African Subtropics. *Mon. Weather Rev.* **1979**, *107*, 620–623. [[CrossRef](#)]
41. Valle, M.A.V.; García, G.M.; Cohen, I.S.; Oleschko, L.K.; Corral, J.A.R.; Korvin, G. Spatial Variability of the Hurst Exponent for the Daily Scale Rainfall Series in the State of Zacatecas, Mexico. *J. Appl. Meteorol. Climatol.* **2013**, *52*, 2771–2780. [[CrossRef](#)]